International Journal of ChemTech Research
CODEN (USA): IJCRGG ISSN: 0974-4290
Vol.7, No.2, pp 539-546, 2014-2015

ICONN 2015 [4th -6th Feb 2015]
International Conference on Nanoscience and Nanotechnology-2015
SRM University, Chennai, India

Microwave Hydrothermal Synthesis and Electromagnetic properties of Nanocrystalline $Y_{3-x}Dy_xFe_5O_{12}$ garnets for microwave antenna applications

T.Ramesh[1]*, P.Raju[2], R.S.Shinde[3] and S.R.Murthy[4]

[1]BVRIT Hyderabad college of engineering for women, Hyderabad, India.
[2]Department of physics, Osmania University, Hyderabad, India.
[3]Ferrite Laboratory, RRCAT, Indore, India.
[4]Geethanjali College of Engineering and Technology, Hyderabad, India

Abstract : Nanocrystalline $Y_{3-x}Gd_xFe_5O_{12}$ (where x=0, 0.2, 0.4, 0.6) garnets were synthesized using microwave hydrothermal (M-H) method by controlling process parameters such as temperature, pressure and pH. Phase structure of all the powders was confirmed by using X-ray diffraction (XRD) from which the crystallite size is found to be in the range of 11-21 nm. The particle size is measured using field effective scanning electron microscopy (FESEM) and it is in the range of 10-19 nm. The synthesized powders were sintered at 1100°C/40 min using microwave sintering method. The sintered samples were characterized by using XRD and FESEM and the obtained grain sizes are in the range of 72-90 nm. Complex permittivity, permeability were measured in the frequency range of 1 MHz to 1.8 GHz. The results show that the present samples possess the good electromagnetic properties with low reflection loss and these properties can be explored for the fabrication of microwave antenna.
Keywords: Microwave Hydrothermal (M-H), Garnet, XRD, Complex permittivity, permeability.

Introduction

The use of ferrites for microwave device applications is a fascinated concept in the field of communication technology [1,2]. The ferrite materials such as yttrium iron garnet ($Y_3Fe_5O_{12}$:YIG), Li and NiCoAl ferrites are successfully used in fabrication of microwave components such as isolators, circulators, phase shifters and miniature antennas operating in a wide range of frequencies (0.1–100 GHz). Out of all, YIG is attracted much attention of researchers due to its inherent properties such as high resistivity and Q value, low dielectric and magnetic losses and narrow ferromagnetic resonance line width in microwave region which corresponds to very low microwave loss[3].However, the desired properties for specific application have been provided by controlling the preparation conditions which in turn control the microstructure or it can be done by the addition of appropriate substitution to the pure YIG.As is well known, the structure of YIG consists of three crystallographic sites {tetrahedral (d), Octahedral (a) and dodecahedral(c)} and all are placed with trivalent metal ions, then we can observe a wide variety of magnetic properties by substituting Y by rare earth metals [4,5] or substituting Fe by other trivalent cations[6, 7] and the same was discussed by several researchers. [4,5] improves

the magnetic properties by substituting Ce^{3+} ions and Nd^{3+}ions in place of Y^{3+} respectively. [8] improved the power handling capability of YIG microwave devices by the substitution of Gd^{3+}.Z. [9, 10] observed the decreasing behaviour of magnetic properties by substituting Dy^{3+}, Sm^{3+} in YIG.

However the synthesis of pure and homogeneous nanocrystalline materials also play a key role to improve the performance of the material. Hence, a variety of methods have been used to synthesize the nanocrystalline YIG including ball mill [11], sol-gel [12], co-precipitation[13]. Among them ball mill method requires higher sintering temperature and the sol-gel process need a careful control of atmosphere and also it utilizes expensive precursors. The co-precipitation process is limited to cation solutions with similar solubility products. In this view, the development of simpler, energy efficient and environment friendly process to synthesis YIG garnet nanocrystals with regular morphology and homogeneous chemical compositions is still an active area of research. In this process, a novel method called microwave-hydrothermal (M-H) method is chosen for the synthesis of YIG[14,16]. The synthesized powders were characterized by using XRD, FESEM and then sintered using microwave sintering method. The effect of Dy^{3+} on complex permittivity and permeability properties were studied over a wide frequency range.

Experimental details

Analytical grades of yttrium nitrate (Y $(NO_3)_3 \cdot 6H_2O$), Dysprosium nitrate (Dy $(NO_3)_3 \cdot 6H_2O$) and ferric nitrate (Fe $(NO_3)_3 \cdot 9H_2O$) were purchased from Aldrich chemical company and used without further purification. Deionised water was obtained from Barnstead RO pure system and was bubbled with high-purity nitrogen for at least 30 min before use. The precursor solution of particular composition was prepared by dissolving and mixing the required amounts of the metal nitrates in stoichiometric ratio of (Y + Dy): Fe = 3:5 in 100 ml of de-ionized water. The mixing of nitrates can be done by using magnetic stirrer with 2500 rpm at room temperature. The complete mixing process completed in 3 hours duration. After dissolving all the reagents in the de-ionized water, aqueous 4mol% solution of NH_4OH was added drop wise to the initial precursors until the desired pH=∼11 value was obtained. Then the prepared solution was transferred into tetraflorometaxil (TFM) vessels and kept in a Microwave-Hydrothermal system (MARS-5, CEM. Corp. Mathews, NC) at 160°C/40 min. After the microwave hydrothermal treatment the obtained solid product was washed several times with ethanol and de-ionized water, and then dried overnight at 60°C. The final powders were weighed and the percentage yields were calculated from the total expected based on the solution concentration and volume and the amount that was actually crystallized. The yield of each reaction was approximately 93-95%.

Assynthesized powders were characterized using XRD (Philips PW-1730 X-ray diffractometer) with Cu-K_α radiation (λ =1.5406A°) and FESEM (ZEISS SUPRA 40 VP) and then the synthesized powders were granulated using 2 wt% poly vinyl alcohol as a binder. Then, the powders were pressed into disks and toroids by applying pressure of 150 MPa for 5 minutes. After the binder was burnt out at 300°C, the compacts were microwave sintered at 1100°C/40 min in the air. The microwave sintering process was carried out using a specially designed applicator and which consists of a domestic microwave oven having an output power level tunable up to a maximum of 800 W and operating frequency of 2.45 GHz. The sintering temperature was measured using a pt-13% pt-Rh thermocouple with an accuracy of ± 1°C. The rate of heating and cooling during the microwave sintering was 20°C/min. The structural and morphological characterization of sintered samples were done by XRD and SEM respectively. The Complex permittivity and permeability properties and reflection loss in (dB) were measured in the frequency range of 1 MHz to 1.8 GHz using Agilent 4291B impedance analyzer.

Results and Discussion

Fig 1 shows the XRD patterns of as synthesized $Y_{3-x}Dy_xFe_5O_{12}$(x=0(MH1), x=0.2(MH2), x=0.4(MH3) and x=0.6(MH4)) powders. The XRD analysis reveals that the synthesized powders possess garnet cubic in structure, exhibiting several prominent peaks. The peaks at 2θ of around 28.90, 32.38, 33.21, 35.57, 39.89, 45.18, 51.15, 53.40 and 59.81were present which ascribed to (400), (420), (332), (422), (521), (611), (444), (640) and (800) diffraction planes of YIG phase(JCPDS card # 89-8186).The XRD patterns also exhibit the minute traces of hematite (γ-Fe_2O_3) (JCPDS card # 89-5894)**,** yttrium orthoferrite ($YFeO_3$) (JCPDS card # 73-1345) and dysprosium orthoferrite ($DyFeO_3$) (JCPDS card # 89-6645).The amount of these phases' increases with an increase of Dy^{3+} concentration and this can be minimized by increasing the microwave reaction

temperature, however for the sake of comparison all the powders were synthesized at the same reaction temperature (160°C).

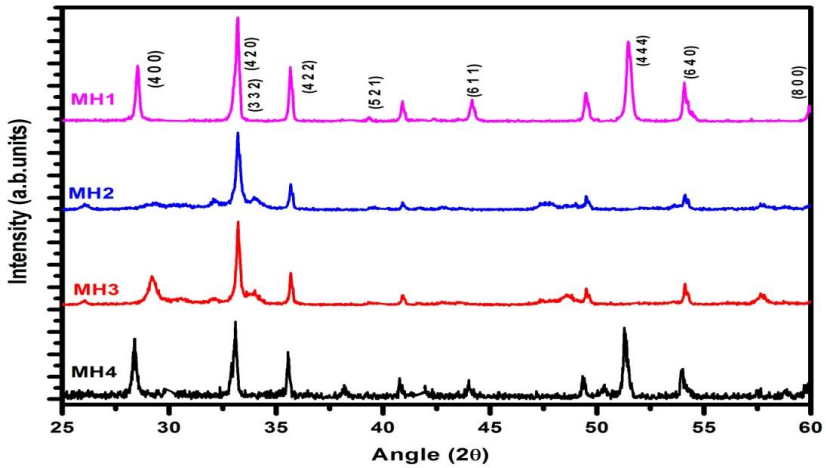

Fig. 1. XRD patterns for as-synthesized MH1-MH4 powders

From the peak broadening of XRD patterns the average crystallite size (D) was calculated using Debye-Scherer formula: $D_m=K\lambda/\beta\cos\theta$, where K (shape factor) is a constant, β is the full width half maxima, λ is the wavelength of X-ray (1.5406 Å) used and θ is the diffraction angle. The average crystallite size obtained from XRD patterns are 11nm, 14nm, 16nm and 18nm for MH1, MH2, MH3 and MH4 respectively. The change in crystallite size is low with Dy^{3+}concentration and it is probably taking place due to the substitution of similar ionic radius Dy^{3+} (0.908Å) in the place of Y^{3+} (0.892 Å) which leads to a minute lattice expansion, which in turn increases the crystallite size is minuscule and the variation has also no apparent regularity.

Fig.2 (a-d) shows the FESEM patterns for the MH1-MH4 powders. It can be seen from the figure that the most of the particles are spherical and well distributed without showing any agglomeration. The particle size is calculated by counting 50 individual particles at various micrographs and taken average. The calculated particle size values are 12nm, 14nm, 15nm and 18nm for MH1, MH2, MH3 and MH4 respectively. It is interesting to find that the Dy^{3+}substitution had no obvious influence on the morphology of the powders. It may be remarked that the observed average particle size values from FESEM patterns is well matched with that of XRD results. The kinetics of the microwave hydrothermal method controls the size of the nano particles and facilitates production of nano particles with narrow size distribution.

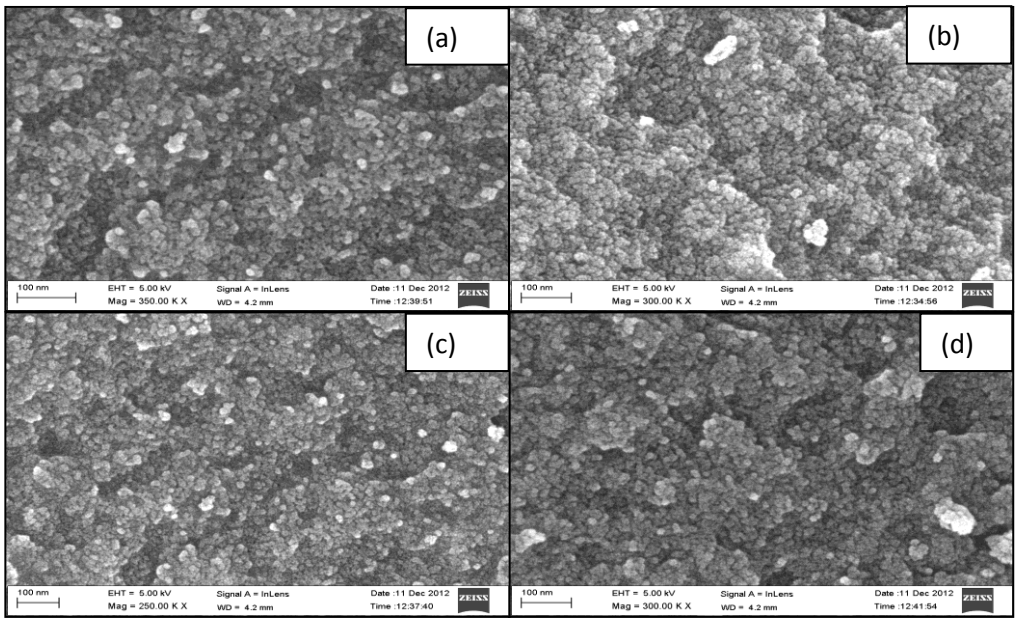

Fig.2 (a-d) shows the FESEM patterns for the MH1-MH4 powders

Fig. 3 shows the XRD patterns for the microwave sintered $Y_{3-x}Dy_xFe_5O_{12}$ samples (where x=0 (MS1), 0.2 (MS2), 0.4 (MS3) and 0.6 (MS4)). It can be seen from the figure that the XRD patterns of Dy^{3+} substituted YIG shows all the major peaks appear essentially at their original position regardless of the substituted concentration i.e. all the present investigated samples shows the single phase structure of the garnet ferrite with good crystallinity and high degree of perfection, whereas no crystal deformation and impurity is observed. It is also observed from the XRD patterns that the 2θ position of each crystal structure shows a slight difference at all with respect to Dy^{3+}substitution implying that the unit cell dimension is changing by Dy^{3+} substitution. The lattice constant "a" of all the Dy^{3+}substituted YIG samples has been determined by usingd value and respective h k l (4 2 0) parameters and the increasing behavior of lattice constant is observed with increase of Dy^{3+} substitution in YIG in the place of Y^{3+}.

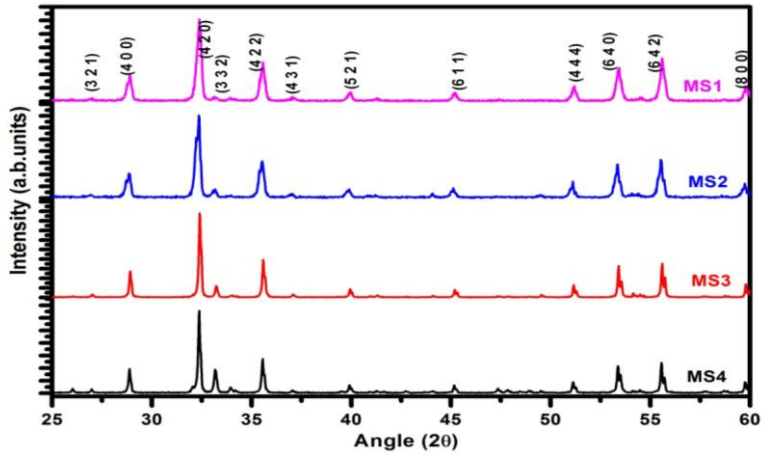

Fig.3. XRD patterns of microwave sintered (MS1-MS4) samples

The X-ray density ($d_{X\text{-}ray}$) for the present investigated samples has been estimated using the relation: $d_{X\text{-}ray}=8M/Na^3$, Where M and N are Molecular weight and Avogadro number respectively, 8 is the number of molecules in the unit cell of garnet lattice and "a" is Lattice constant and the obtained results were presented in Table.1. It can be observed from the table that the X-ray density increases with an increase of Dy^{3+} concentration in YIG. The bulk density (d_{bulk}) of all the samples has been measured accurately using Archimedes principle and obtained results were given in Table.1. It can be seen from the table that the bulk density of the samples linearly increases with an increase of Dy^{3+} concentration in YIG. The increase in d_{bulk} is attributed to increase in mass overtakes the increase in volume of the unit cell. In the microwave sintering process, temperature rises to 1100°C within 40 min and attains high theoretical density (TD) of 91-94%. Thus, higher densification has been achieved in shorter period using the microwave sintering process.The porosity (P) of the samples has been estimated using the equation: P % = [1-(Bulk density/X-ray density)] x 100 and the obtained values are in the range of 6 - 9%.

Unlike in the conventional sintering, the microwave sintered samples show improved crystallinity even at a low sintering temperature 1110°C. The line width observed in the XRD pattern is narrower than that of the line widths of the corresponding as synthesized nanocrystalline powders. However, all the samples show nanocrystalline nature after microwave sintering also and there is no distorted structure observed for the present investigated microwave sintered samples.

Fig.4 (a-d) shows the SEM micrographs for all the microwave sintered samples (MS1-MS4). It can be seen from the figure that the samples exhibit quasi round in shape and quite uniform in size. The average size of the garnet grain, geometrically estimated from SEM micrographs using linear intercept methods by taking average of fifty grains and obtained values are given in Table 1. As is shown by the results, microwave sintering favors the development of coarser polycrystalline microstructure when compared to conventional sintering. The controlling heating rate of the microwave firing process moves over the coarser the microstructure or the smaller increasing of the average grain size. In the microwave sintering process, the local temperature differences in pores and interfaces in the earlier stage of sintering are considered to be the origin of the microwave effect[17]. The microwave radiation effect on grain growth is expected to be smaller than the effect on densification in the case of densified sample as these interfaces disappear in the later stage of sintering. As a consequence enhanced grain growth is not observed with isothermal microwave heating[18]. Due to this reason microwave sintered samples possesses small and uniform grains.

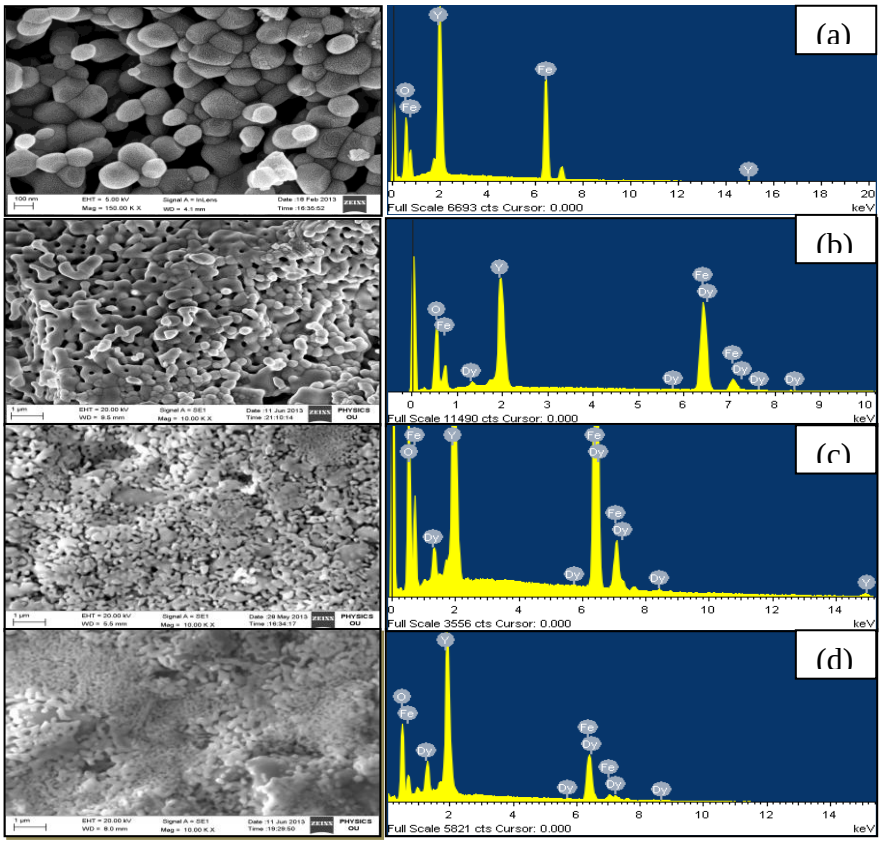

Fig.4. SEM &EDS patterns for the microwave sintered (MS1-MS4) samples

The EDS of the corresponding samples shows the existence of Y, Dy, Fe and Oxygen elements and without showing any extra unwanted elements. The elemental ratios were within the experimental error (1-2%) identical for the same sample across many surface spots indicating that a homogeneous sample was formed. By EDS it was found that the obtained atom percentages are very close to the starting composition. Thus, high purity samples can be obtained by M-H method. The applicability of a material for a particular device is tested by appropriate properties in different conditions. In the same way the performance of the ferrites can be estimated from the studies of dependence of permeability on the frequency. Fig.5 shows the complex permeability for the microwave sintered MS1-MS4 samples in the frequency range of 1MHz to 1.8 GHz. In general, the complex permeability spectra of polycrystalline ferrites depends on the chemical composition, sintering density and the microstructure such as grain size, porosity and intragranular pores. In the present investigation, the porosity and grain size of all samples does not show much variation with Dy^{3+}substitution; therefore in the present situation the complex permeability mainly depends on the chemical composition of the sample. From the figure, it can be observed that the real part of the permeability remained almost constant, until the frequency was raised to a certain value, and then began to decrease at higher frequency. The imaginary permeability gradually increased with the frequency, and reached a broad maximum at a certain frequency, where the real permeability rapidly decreased. This feature is mainly arises due to the domain wall relaxation[19, 20]. The measured real (μ') and imaginary (μ") part of permeability values at 1MHz were given in Table.1. From the table, it can be observed that the real permeability decreases from 227 for pure YIG to 163 for $Y_{2.4}Dy_{0.6}Fe_5O_{12}$ and the imaginary permeability (μ') is for all the samples is in the order of 10^{-2}. The observed reduction in μ' with Dy^{+3} substitution can be explained as follows. The initial permeability is proportional to the square of saturation magnetization[21]. Hence, the variation of initial permeability with dysprosium substitution follows a similar trend to that of saturation magnetization.

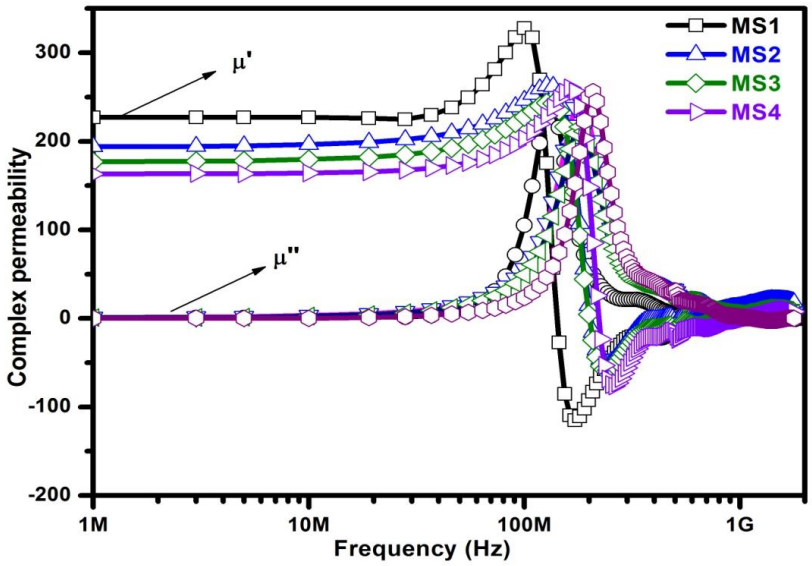

Fig.5. Complex permeability spectra for the microwave sintered MS1-MS4 samples

Fig. 6 gives the frequency dependence of the real (ε') and imaginary (ε") parts of permittivity at room temperature. It can be seen from the figure that the values of ε' and ε" for present ferrites are low and remain constant as the frequency increases from 1MHz to 800MHz. With further increase of frequency, the values of ε' and ε" increase with an increase of frequency and shows a resonance at 1.4 GHz. This behaviour of frequency dependence of ε' can be understood with the help of hopping mechanism [19, 22].

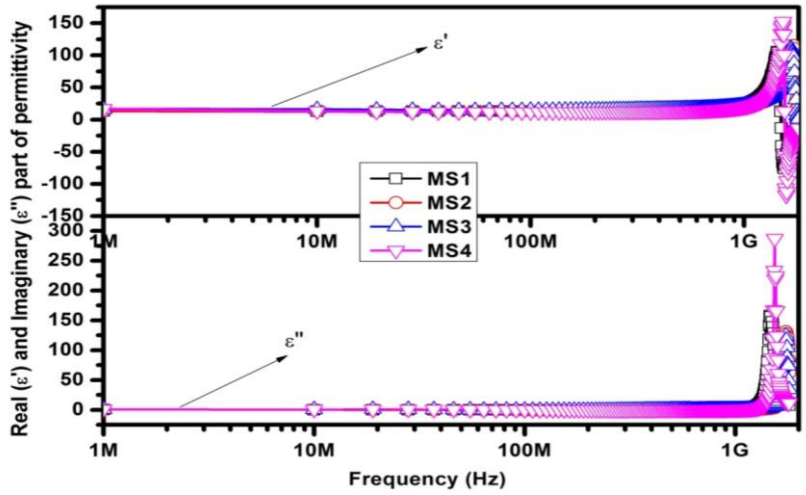

Fig. 6. Frequency dependence of the real (ε') and imaginary (ε") parts of permittivity

Table.1: Structural, magnetic and dielectric properties of microwave sintered samples

Sample	Lattice constant (Å)	d_{bulk} (g/cc)	$d_{X\text{-}ray}$ (g/cc)	Porosity (%)	μ' at 1MHz	μ'' at 1MHz	ε' at 1MHz	ε'' at 1MHz
MS1	12.387	4.97	5.15	4	227	1.02	15.4	0.004
MS2	12.391	5.07	5.28	4	194	1.10	16.3	0.014
MS3	12.392	5.15	5.40	5	177	0.80	17.5	0.018
MS4	12.397	5.23	5.52	5	163	1.08	17.9	0.026

Reflection loss for the MS1-MS4 samples was measured and shown in Fig. 7. It can be seen from the figure that the present investigated samples shows a measured resonance frequency of around 300MHz-500MHz. The reflection loss varies from sample to sample and it is low for MS1 and high for MS3. The larger reflection loss, and wider bandwidths is possible in the present investigated samples is due to their uniform grain morphology and small grain size close to the single-domain.A shift of RL peaks towards higher frequencies has been observed with increase of Dy^{3+} substitution.

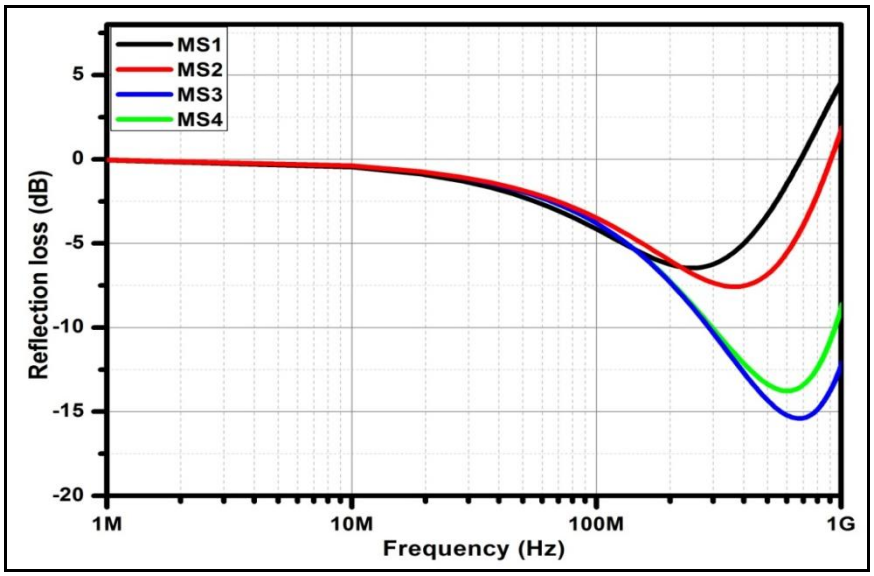

Conclusions:

Nanocrystalline $Y_{3-x}Gd_xFe_5O_{12}$ powders were successfully synthesized using M-H method. The alkalinity, reaction temperature and reaction time of the synthesis play key roles in influencing the crystallization and composition of the products. The samples were densified at a low temperature 1100°C/40 min using microwave sintering method. Substitution of Dy^{3+} in place of Y^{3+} in YIG affects the structural, magnetic and electrical properties. All the investigated samples exhibit low magnetic and dielectric losses over a wide frequency range. Reflection loss and resonance frequency increases with increase Dy^{3+} concentration. Thus, a suitable combination of ferrite composition and the processing technique results in a prospective material for the desired application. The properties of the investigated samples guide us to apply these compositions to fabrication of microwave antenna in the lower microwave region.

Acknowledgement:

One of the authors (T.Ramesh) would like to thank CSIR for providing SRF fellowship.

References

1. Fechine, P.B.A., Rocha, H.H.B., Moretzsohn, R.S.T., Denardin, J.C., Lavın, R., Sombra, A.S.B; Study of a microwave ferrite resonator antenna, based on a ferrimagnetic composite $(Gd_3Fe_5O_{12})GdIG_X$–$(Y_3Fe_5O_{12})YIG_{1-X}$; IET Microw. Antennas Propag., 2009, 3; 1191– 1198
2. Vincent, G., Harris, et.al.,Recent advances in processing and applications of microwave ferrites,J. Magn. Magn. Mater., 2009, 321;2035-2047.
3. Pardavi-Horvath, M.,Microwave applications of soft ferrites, J. Magn. Magn. Mater. 2000, 215; 171-183.
4. Haitao, Xu., Hua, Yang., Wei, Xu., Shouhua Feng,Magnetic properties of Ce,Gd-substituted yttrium iron garnet ferrite powders fabricated using a sol–gel method J. Mater. Process. Technol, 2008, 197; 296–300
5. Zhongjun Cheng., Hua Yang.,Magnetic properties of Nd-$Y_3Fe_5O_{12}$ nanoparticles, J. Mater. Sci. - Mater. Electron.2007,18;1065–1069
6. Tongmee,S., Winotai,P., Tang. I.M; Local field fluctuations in the substituted aluminium iron garnet $Y_3Fe_{5-x}Al_xO_{12}$; Solid State Commun. 1999,109; 471-476.
7. AzadiMotlagh,Z., Mozaffari,M., Amighian,J., Lehlooh,A.F., Awawdeh,M., Mahmood,S., Mossbauer studies of $Y_3Fe_{5-x}Al_xO_{12}$nanopowders prepared by mechanochemical method;Hyperfine Interact. 2010, 198; 295-302
8. Bijoy, K., Kuanr.,Effect of rare-earth Gd^{3+} on instability threshold of YIG,J. Magn. Magn. Mater.,1997,170; 40-48
9. Zhongjun Cheng., Hua Yang., Yuming Cui., Lianxiang Yu., Xueping Zhao., Shouhua Feng., Synthesis and magnetic properties of $Y_{3-x}Dy_xFe_5O_{12}$ nanoparticles, J. Magn. Magn. Mater., 2007, 308; 5-9

10. Zhongjun Cheng., Hua Yang., Synthesis and magnetic properties of Sm–$Y_3Fe_5O_{12}$ nanoparticles, Physica E, 2007,39; 198–202
11. Ristic, M., Nowikb, I., Popovic, S., Felner, I., Music, S., Influence of synthesis procedure on the YIG formation; Mater. Lett. 2003, 57; 2584-2590
12. HosseiniVajargah, S., MadaahHosseini, H.R, Nemati, Z.A.,Mater. Sci. Eng., B,2006, 129; 211–215.
13. Rashad, M.M., Hessien, M.M., El-Midany, A., Ibrahim, I.A., Effect of synthesis conditions on the preparation of YIG powders via co- precipitation method, J. Magn. Magn. Mater., 2009, 321; 3752–3757.
14. Sridhar Komarneni., Rustum Roy, Li.Q.H., Microwave-hydrothermal synthesis of ceramic powders, Mater. Res. Bull.,1992, 27; 1393-1405
15. Ramesh,T., Shinde,R.S., Murthy,S.R., Synthesis and characterization of nanocrystalline $Ni_{0.94}Co_{0.03}Mn_{0.04}Cu_{0.03}Fe_{1.96-x}Al_xO_4$ ferrites for microwave device applications, J.Magn. Magn. Mater., 2013, 345; 276-281.
16. Ramesh, T., Shinde, R.S., Murthy, S.R., Nanocrystalline gadolinium iron garnet for circulator applications, J.Magn. Magn. Mater., 2012, 324; 3668-3673.
17. Sutton, W.H., Microwave Processing of Ceramic Materials, Am.Ceram.Soc.Bull., 1989, 68; 376-385.
18. Saita, H., Fang, Y., Nakano, A., Agrawal, D., Lanagan, M., Shrout, T.R., Randall, C.A., Microwave Sintering of NiCuZn Ferrite Ceramics and Devices,Jpn.J.App.Phys. 2002, 41; 86-92.
19. Ramesh, T., Shinde, R.S., and Murthy, S.R., Synthesis and characterization of $NiCoMnCuFe_{1.96}O_4$ for circulator application, J.Magn. Magn. Mater., 2011, 323; 1593-1598.
20. T. Nakamura., Low-temperature sintering of NiZnCu ferrite and its permeability spectra, J. Magn. Magn. Mater., 1996, 168; 285-291.
21. Went, J.J., and Wijn, H.P.J., The Magnetization Process in Ferrites, Phys. Rev. 1951, 82; 269.
22. Verma, A., Goel, T.C., Mendiratta, R.G., Alam, M.I., Dielectric properties of NiZn ferrites prepared by the citrate precursor method, Mater. Sci. Eng. B 1999, 60, 156-162.
23. K, Praveena., K, Sadhana., S, Bharadwaj., S.R. Murthy., Development of nanocrystalline Mn–Zn ferrites for high frequency transformer applications, J. Magn. Magn. Mater, 2009,321; 2433.

*****